

The 24 Aqr triple system: A closer look at its unique high-eccentricity hierarchical architecture

Ahmad Abushattal¹, Mashhoor A. Al-Wardat^{2,3}, Elliott P. Horch⁴, Nikolaos Georgakarakos^{5,6}, Hatem A. Al-Ameryeen¹, Enas M. Abu-Alrob³, and Abdallah M. Hussein³¹

¹Department of Physics, Al-Hussein Bin Talal University, PO Box 20, 71111, Maan, Jordan

²Department of Applied Physics and Astronomy, and Sharjah Academy for Astronomy, Space Sciences and Technology, University of Sharjah, PO Box 27272, Sharjah, UAE

³Department of Physics, Al al-Bayt University, Mafraq 25113, Jordan

⁴Department of Physics, Southern Connecticut State University, 501 Crescent Street, New Haven, CT 06515, USA

⁵Division of Science, New York University Abu Dhabi, Abu Dhabi, UAE

⁶Center for Astrophysics and Space Science (CASS), New York University, Abu Dhabi, PO Box 129188, Abu Dhabi, UAE

December 30, 2025

Abstract

As its periastron passage occurred during the third quarter of 2020, system 24 Aqr is of particular significance. New visual solutions for the latest speckle interferometry observations collected by the Lowell Discovery Telescope (LTD) with its new QWSSI speckle camera are presented here. A variety of techniques were used to analyze the system, including ORBITX code for orbital solution, Al-Wardat's method for analyzing multiple stellar systems, and Edwards' method for analyzing visual and spectroscopic binaries. We derive precise masses and the complete set of its fundamental parameters for the three components, and we introduce a new orbital solution, and a new dynamical parallax, which is very close to the measured value given by Hipparcos 2007 and from that of Gaia DR2. In the next section, we discuss the possibility of a coplanar orbit. In conclusion, we demonstrate that we need a 65-m telescope to resolve the inner binary visually, although an array of telescopes could be used instead.

Keywords: Stars: binaries: close; Hierarchical Triple System; Visual Binary Stars; Spectroscopic Binary Stars; Multiple stars; Observational Astronomy; Atmospheric Modeling-Synthetic Photometry

1 Introduction

The study of multiple stellar systems has gained special importance over time because of its influence on understanding the stellar formation and evolution theories. The rapid development of the observational tools and the availability of data provided by astronomical missions such as Gaia, Hipparcos, and Kepler, helped to reveal the properties of such systems (Perryman et al., 1997; Van Leeuwen, 1997; Prusti et al., 2016). The prime objective of the Kepler mission was to search for Earth-like planets, but it also detected eclipses in multiple systems (Carter et al., 2011; Abushattal et al., 2019; Abushattal et al., 2022a; Abushattal et al., 2022b). More than 50% of the stars in the galaxy are believed to be binary or multiple systems, with 46% of them having at least one companion, and more than 30% are multiple stellar systems with a binary star as one of the components (Stassun, 2012; Tokovinin, 2014b). During the past decades, many studies have used high-resolution techniques to investigate those binaries. Those efforts provided the most appropriate methods for calculating and determining orbital parallaxes and stellar masses by using the correlation between the visual and spectroscopic orbits (Bonneau et al., 1980; Balega and Ryadchenko, 1984; Fekel et al., 1997; Al-Wardat et al., 2017; Docobo et al., 2017; Mendez et al., 2018; Tokovinin, 2018; Docobo et al., 2018a; Docobo et al., 2018b).

Many multiple systems are hierarchical triples (Abu-Alrob et al., 2023). They can be perceived as being comprised of two subsystems: a single star (the outer star) that orbits widely around the center of mass of a binary system (inner binary) with $a_{out} >> a_{in}$, a_{out} and a_{in} being the semi-major axis of the outer and inner orbit respectively. The evolution of such systems is governed by various astrophysical processes taking place among its members, such as for example mass transfer, tidal friction, and gravitational interactions (e.g. see Georgakarakos, 2002; Fabrycky and Tremaine, 2007; Toonen et al., 2020; Naoz et al., 2013; Taani et al., 2019a; Taani et al., 2019b). Triple systems can help us understand star formation and evolution during the various phases. Fekel (1981), Vynatheya et al. (2022), Georgakarakos (2005) published the first list of hierarchical systems. Since then, several observational efforts have been made to study that kind of system (e.g. Fekel et al., 1997; Derekas et al., 2011; Tokovinin, 2014b; Tokovinin, 2014a).

The system 24 Aqr consists of a close spectroscopic binary (SB) and a third star on a much wider orbit. 24 Aqr was known to be a triple as early as 1963 (Eggen, 1963), where it was also suggested that the system's total mass was $1.51M_{\odot}$. Based on the variability of the system's radial velocity measurements, the same conclusion regarding the triple nature of the system was reached by Heintz (1981). Later on, Lippincott (1982) suggested a $0.73 \pm 0.20M_{\odot}$ star for the primary component, while the secondary component was $0.76 \pm 24M_{\odot}$. Based on the amplitude of the radial velocity curve, Griffin et al. (1996) determined that the masses of the two components of the spectroscopic pair were $1.19M_{\odot}$ and $0.15M_{\odot}$, while the mass of the distant visual component was $1.10M_{\odot}$. The spectral type of the system has been another subject of investigation. In the Henry Draper Catalogue, the spectral type is F8V (Cannon and Pickering, 1924), while it is F7V in Christy and Walker (1969), and F8V in Harlan (1974). In SIMBAD, the F6V classification was determined by Abt (1985), Wenger et al. (2000). Griffin et al. (1996) also studied this system and by combining the relative dip area of the radial velocity based on spectroscopic observation and the color index $B - V$, they suggested that the spectral type for 24 Aqr was F8V, with F7V for the primary component of the spectroscopic binary and F9.5 V for the secondary.

The orbit of the visual binary has also been under investigation for over 100 years. Initially, Kuiper (1926) determined the orbital period to be 71 years with an eccentricity of 0.893. Subsequently, Finsen (1929b) gave a 51.33-year period with a 0.910 eccentricity, and then Aitken (1932) brought the period down to 46.6 years and the eccentricity to 0.85. A few years later, Mannino (1946) proposed a much higher value of 99.46 years but with an eccentricity of 0.25. In more recent

years, Griffin et al. (1996) found an orbit with a period of 48.7 years and an eccentricity of 0.86. Finally, in 2019, Tokovinin published the orbital solution in double stars information circular No. 199 with a period of 48.67 years, based on observations of (Aitken and Millard, 1932; Finsen, 1929a; Danjon, 1942; Mannino and Humblet, 1955; Heintz, 1997; Scardia et al., 2019). Table 2 lists the orbital elements for the visual orbital solutions mentioned above.

In this work, we reanalyze the system 24 Aqr, also known as HD 206058 using the latest available data. We attempt to determine as accurately as possible the physical and orbital parameters of the 24 Aqr triple system. We make use of all available data, spectroscopic and astrometric observations, and derived orbital solutions of the system. We shall apply two different methods. First, we use Edwards' method in order to determine the individual masses and spectral type of both components of the spectroscopic binary (Edwards, 1976; Abushattal et al., 2020). Subsequently, we use the Al-Wardat method which is an atmospheric modeling and synthetic photometry method with the aim of determining the physical parameters of the system (Al-Wardat, 2003b; Al-Wardat, 2007; Al-Wardat, 2008; Al-Wardat and Widyan, 2009; Al-Wardat et al., 2014; Masda et al., 2019; Al-Wardat et al., 2021b; Hussein et al., 2022).

Then, by combining the results of both methods, we get the complete solution for the 24 Aqr triple system and we are able to determine the most probable 3D orbit for the system. Furthermore, we discuss the possibility of coplanarity of the system using all information at our disposal from both the spectroscopic and visual binary orbits. The structure of the paper is as follows: in Section 2 we analyze the main component (A) of this triple system as a spectroscopic binary using Edwards' process and atmospheric modeling and synthetic photometry. In Section 3 we discuss the orbital alignment of the two orbital planes, while in Section 4 we investigate whether we can resolve the spectroscopic binary component (A) visually. Finally, in Section 5, we present our conclusions.

2 Analysis of system

2.1 The visual orbit

The orbital properties for the main system of 24 Aqr were determined using the dynamical technique developed by Tokovinin et al. (2016). This method uses the least-squares fits with weights inversely proportional to the observational errors to give the final orbital parameters with their errors using ORBITX code with IDL. We used relative position measurements from speckle interferometric observations to determine the visual orbit. We obtained most of the positional measurements for the system from the Fourth Catalog of Interferometric Measurements of Binary Stars (Hartkopf et al., 2010). However, four new measurements, used for the first time in this work, were taken with the QWSSI speckle instrument (Clark et al., 2020) at the Lowell Discovery Telescope on 27 Aug 2021 UT. These were especially important to the visual orbit calculation as they were close to the periastron passage. The full list of measures used is shown in Table 1. Fig. 1 shows the modified orbit of 24 Aqr. We used seven new measurements to improve the orbital solution of the main orbit of the system. The new measurements covered the periastron passage which raised the orbit Grade from 2 to 1. A zero residual signifies an exact match with the orbit. We therefore assign zero uncertainty to separation uncertainties for certain data points, while uncertainty for position angle is not taken into account when calculating orbital elements.

2.1.1 The Spectroscopic Binary Component (A)

In this section, we determine the three-dimensional orbit for the SB components and we estimate the most probable values of the physical parameters of this system such as the magnitude, spectral type,

and masses. For the single-lined spectroscopic binary, we know the following orbital parameters: the period P, the epoch of the periastron T, the eccentricity e, $A_1 = a_1 \sin(i_S)$ (a_1 is the semi-major axis of the orbit for the main component), the inclination i_S , the argument of periastron χ corresponding to the orbit of the main component and the mass function $f(m)$. In addition, we know the composite spectrum, the apparent global magnitude, and the parallax (Hipparcos or Gaia parallax). The initial data for 24 Aqr can be found in Table 3.

Using Edwards' method, we start from the transformation of the apparent magnitude to the absolute magnitude and then we apply Edward's process in order to determine the individual spectrum for each star depending on the difference of the magnitude D_m (Edwards, 1976; Abushattal et al., 2020; Docobo et al., 2017). We can also determine the masses of each component, since, due to the improvement in observational methods in the last decades, the accuracy in the masses has increased significantly. Hence, we estimate the masses depending on the different calibrations done by (Straižys and Kuriliene, 1981; Malkov, 2007; Docobo and Andrade, 2006; Pecaut and Mamajek, 2013). Afterwards, we calculate the semi-major axis of the relative orbit a and the two semi-major axes of the barycentric orbits a_1 and a_2 in (A.U). Finally, from the semi-major axes, and using the mass function, we can determine the inclination, i_S .

2.2 Atmospheric Modeling and Synthetic Photometry

One of the most effective methods for the analysis of such systems is the novel computational spectrophotometric method known as Al-Wardat's method for analyzing multiple systems (MSs) (Al-Wardat, 2002; Al-Wardat, 2012), which was successfully applied in the analysis of several main-sequence and subgiant BMSs (Al-Wardat, 2003b; Al-Wardat, 2003a; Al-Wardat, 2007; Al-Wardat, 2012; Al-Wardat et al., 2014; Masda et al., 2019; Al-Wardat et al., 2021a; Hussein et al., 2022; Tanineah et al., 2023). The idea of the method in brief is to use the measured visual magnitude m_V and a color index $B - V$ of the entire system along with the visual magnitude difference between their components to estimate the complete set of their physical and atmospheric parameters. It is difficult to measure the spectra for each component of MSs, where the components are close to each other and exhibited as one star in large telescopes. In order to get the entire synthetic SED of the system which is related to the energy flux of the components located at a distance d (pc) from the Earth, we use the following equation Al-Wardat (2002):

$$F_\lambda \cdot d^2 = (H_\lambda^{Aa} \cdot R_{Aa}^2 + H_\lambda^{Ab} \cdot R_{Ab}^2) + H_\lambda^B \cdot R_B^2 \quad (1)$$

where F_λ is the flux for the entire synthetic SED of the entire binary system at the Earth, H_λ^{Aa} , H_λ^{Ab} and H_λ^B are the fluxes of the primary and secondary components, while R_{Aa} , R_{Ab} and R_B are the radii of the primary and secondary components in solar units R_\odot .

It employs Kurucz (ATLAS9) line-blanketed plane-parallel model atmospheres to build the fluxes for the individual components (Kurucz, 1994d) and atomic data provided later on (Kurucz, 1994a; Kurucz, 1994c; Kurucz, 1994b; Kurucz, 1994e). In order to apply the method, we need the magnitude difference between the components of the system, which was measured for the main two components A and B using speckle interferometry, and for the two sub-components Aa and Ab through the spectroscopic analysis in this work as Edwards' process from Table 6. The synthetic spectral energy distributions (SEDs) for the entire and individual components are shown in Fig. 2 (left one). Moreover, the results of synthetic photometry for Johnson-Cousins ($UBVR_C$) filters, Strömgren (ubvy) filters and Tycho filters (B_T, V_T) for synthetic SEDs and color indices are listed in Table 4. The atmospheric parameters and other calculated fundamental parameters are listed in Table 5. Fig. 2 shows the positions of the components on the evolutionary tracks and isochrones Girardi et al. (2000).

Where the metalicity Z can be calculated using measurements of Iron abundance relative to the Sun $[Fe/H]$ using the following equation:

$$\log Z = 0.977[Fe/H] - 1.699 \quad (2)$$

According to Gaspar et al. (2016), the metalicity abundance is $[Fe/H] = -0.08 \pm 0.07$, leading to a value of metalicity $Z = 0.017$ which is close to the Sun metalicity $Z = 0 : 019$.

The positions of the components in the isochrone at 3.612 Gyr indicate that all three components are main sequence stars. However, the first component is transitioning from the main sequence stage to the subgiant stage. Fragmentation seems to be the most probable mechanism for the system's formation.

In accordance with Al-Wardat's method, which is unaffected by variations in parallax measurements (see Table 7), the most accurate estimate of the system's mass sum is $2.39 \pm 0.18 M_{\odot}$ Al-Wardat et al. (2021b); Hussein et al. (2023). By combining modified orbital parameters for the system with calculated mass sum using Al-Wardat's method, we can calculate a new dynamical parallax for the system using the following equations:

$$3 \log(\pi_{Dyn}) = 3 \log h - \log(\Sigma M) \quad (3)$$

where $\log(h) = \log(a) - \frac{3}{2} \log(P)$. This yields a new dynamical parallax of ($\pi_{Dyn} = 23.75 \pm 0.25 mas$), close to Hipparcos value ($22.74 \pm 0.81 mas$). There is an unusually large error in Gaia DR2, but DR3 does not resolve the components and does not include a parallax update. We will have to wait until DR4 is released. Thus, one of the unique aspects of our analysis is our dynamical parallax, which is at present the most precise value available.

2.3 The Edwards process

Christy and Walker (1969) established individual MK classifications for both components using MK spectral class decompositions. As per Terry W. Edwards's procedure, a standard luminosity calibration for the MK system is employed with a minor modification A composite type can be formed by linearly interpolating the MK spectral types of the individual binary components, weighted by their luminosities (Blaauw and Strand, 1963; Christy and Walker, 1969; Schmidt-Kaler, 1965; Edwards, 1976). This method is of interest for studying the stellar properties of binary stars and their exoplanets. An extremely valuable feature is its simplicity and dependence on apparent size and parallax (Abushattal, 2017; Abushattal et al., 2020; Al-Tawalbeh et al., 2021; Anguita-Aguero et al., 2022; Videla et al., 2022; Chauvin et al., 2022). As a result, the masses and spectral types of stellar stars are close to those calculated by other astrophysical methods. In this method, we can predict the physical properties of the orbital elements and the orbital differences. In addition, we can predict the individual mass of spectral binaries by simultaneously fitting the optical orbit and radial velocity curves. Since the SB1 systems only display the spectral lines of the primary object, the mass of primary object can also be estimated experimentally (Abushattal et al., 2020; Anguita-Aguero et al., 2022). In the presence of partial and in-homogeneous observations, it provides accurate and efficient estimation of the joint posterior distribution of orbital parameters. The Bayesian inference methodology for parameter estimation is computed by integrating this method with the Markov chain Monte Carlo algorithm (Abushattal et al., 2020). This method was used to calculate the 3D orbits of SB1, SB2, and confirming data extracted by other methods regarding stellar masses and spectral types. This provided additional external information allowing us to mitigate the problem of not determining the mass ratio as well (Anguita-Aguero et al., 2022). On the other hand, it helps to understand the structures for testing predictions of planet formation and evolution theories in binary

Table 1
The positional measurements with residuals.

Epoch	Theta (θ°)	Rho (ρ'')	$\delta\rho$	$(O - C)_\theta$	$(O - C)_\rho$	Ref.
1923.882	333.5	0.152	0.9	165.7	0.023	Mag1925
1978.618	226.1	0.275	0.019	0.5	-0.004	McA1980b
1980.723	236.3	0.323	0.004	1.6	-0.001	McA1983
1980.909	236.5	0.333	0.005	1.1	0.005	Tok1982a
1981.474	236.5	0.337	0.01	-0.9	-0.002	McA1984a
1981.703	239.2	0.339	0.01	1	-0.004	McA1984a
1982.508	243	0.346	0.01	2.3	-0.012	Hrt2000a
1982.531	240.9	0.345	0.01	0.1	-0.014	McA1997
1982.763	242.5	0.354	0.01	1	-0.009	McA1987b
1983.713	246.1	0.377	0.01	1.9	-0.003	McA1987b
1985.752	253	0.398	0.015	3.7	-0.016	Tok1988
1985.848	251.6	0.405	0.01	2.1	-0.01	McA1987b
1986.891	252.7	0.430	0.01	0.9	-0.001	Hrt2000a
1987.754	254.5	0.445	0.01	0.9	0.002	McA1989
1988.666	257	0.458	0.09	1.6	0.003	Hrt2000a
1989.613	259.3	0.463	0.09	2.2	-0.004	McA1997
1989.717	258.8	0.467	0.09	1.5	-0.001	Hrt1992b
1990.344	260.1	0.470	0.09	1.7	-0.005	Hrt1993
1991.25	261.1	0.482	0.09	1.1	-0.003	HIP1997a
1991.6	263.9	0.540	0.9	3.3	0.051	TYC2002
1991.713	262	0.485	0.09	1.2	-0.005	Hrt1996b
1991.747	264.2	0.510	0.1	3.4	0.02	WSI1997
1992.7	262.5	0.470	0.09	0.2	-0.029	WSI1997
1992.7	263.6	0.460	0.09	1.3	-0.039	WSI1997
1992.705	264.8	0.50	0.01	2.4	0.001	WSI1997
1992.705	263.6	0.510	0.01	1.2	0.011	WSI1997
1992.765	263.3	0.510	0.01	0.9	0.01	WSI1997
1992.823	263.1	0.490	0.01	0.6	-0.01	WSI1997
1992.877	263.9	0.510	0.09	1.3	0.009	WSI1997
1993.661	266.6	0.490	0.01	2.8	-0.018	WSI1999a
1993.697	264.5	0.490	0.01	0.6	-0.018	WSI1999a
1993.817	264.9	0.490	0.01	0.8	-0.019	WSI1999a
1993.893	265.9	0.510	0.045	1.7	0.001	WSI1999a
1994.519	266.6	0.531	0.01	1.5	0.017	Hor2006c
1994.519	266.1	0.527	0.01	1	0.013	Hor2006c
1994.679	265.5	0.500	0.045	0.1	-0.015	WSI1999a
1994.701	266.3	0.510	0.01	0.9	-0.006	WSI1999a
1994.708	266.5	0.513	0.009	1.1	-0.003	Hrt2000a
1994.764	266.8	0.510	0.08	1.3	-0.006	WSI1999a
1994.764	266.1	0.510	0.06	0.6	-0.006	WSI1999a
1994.816	263.4	0.470	0.01	-2.2	-0.046	WSI1999a
1994.816	262.8	0.480	0.1	-2.8	-0.036	WSI1999a
1995.662	267.7	0.480	0.01	0.9	-0.042	WSI1999b
1995.662	266.6	0.510	0.01	-0.2	-0.012	WSI1999b
1995.682	266.6	0.510	0.01	-0.2	-0.012	WSI1999b
1995.753	267.8	0.510	0.045	0.9	-0.013	WSI1999b
1995.762	268.2	0.514	0.01	1.2	-0.009	Hrt1997
1995.772	267.7	0.480	0.045	0.7	-0.043	WSI1999b
1996.535	269	0.519	0.1	0.9	-0.008	Hrt2000a
1996.749	268.1	0.520	0.045	-0.3	-0.008	Hor1999
1997.521	269.6	0.541	0.008	0.2	0.009	Hor1999
1997.613	271.2	0.527	0.01	1.6	-0.005	WSI1999c
1999.781	273.5	0.540	0.009	1	0.001	Hor2000
1999.782	273.6	0.520	0.009	1.1	-0.019	WSI2000b
1999.885	273.4	0.530	0.009	0.7	-0.009	Hor2002a
2000.751	275	0.510	0.009	1.2	-0.03	WSI2001b
2001.719	275.7	0.530	0.009	0.5	-0.01	WSI2002
2004.955	280.1	0.528	0.004	0.5	-0.004	Sca2006d
2006.559	280.9	0.523	0.009	-0.9	0.001	Hrt2009
2008.543	284.9	0.505	1E-4	0.1	0	Tok2010
2008.549	284.9	0.505	0	0.1	0	Tok2010
2008.767	285.1	0.502	0	0	0	Tok2010

(continued on next page)

Table 1 (continued)

Epoch	Theta (θ°)	Rho (ρ'')	$\delta\rho$	$(O - C)_\theta$	$(O - C)_\rho$	Ref.
2015.743	299.5	0.359	0	0	0	Tok2016a
2015.743	299.5	0.359	0	0	0	Tok2016a
2017.6006	306.6	0.2844	1E-4	0.1	0.002	Tok2018
2018.5617	312.1	0.2299	1E-4	-0.1	0.001	Tok2019
2019.3753	320.1	0.1703	2E-4	-0.1	0.001	Tok2020
2019.5394	322.2	0.1564	1E-4	-0.4	0.001	Tok2020
2020.8229 **	88.4	0.0398	1E-4	-7.1	-0.002	Tok2021
2021.3195 **	144.9	0.0879	1E-4	-0.6	-0.001	Tok2022
2021.5654 **	156.6	0.1029	4E-4	1	-0.002	Tok2022
2021.655 **	159.7	0.112	0	1.1	0.001	This work
2021.655 **	157.4	0.110	0	-1.2	-0.001	This work
2021.655 **	153.7	0.111	0	-4.9	0	This work
2021.655 **	158.8	0.110	0	0.2	0	This work

** measurements used for first time.

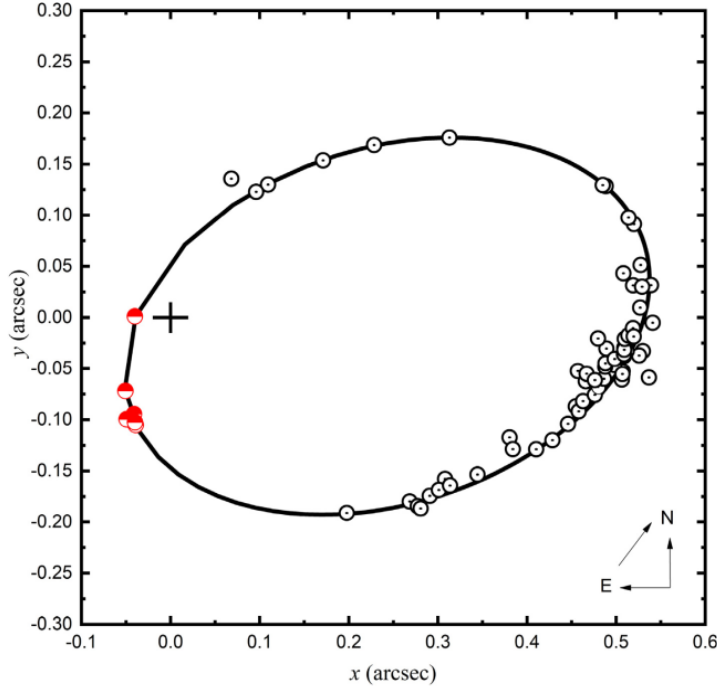


Fig. 1. The apparent orbit of 24 Aqr system as determined from our analysis.

Table 2

The astrometric orbit of 24 Aqr. P is the period in years, T is the epoch of the periastron passage, e , is the eccentricity, a is the semi-axis major in arc seconds, the argument of periastron ω , i_L , is the inclination and finally Ω is the longitude of the node.

Author	P (yr)	T	e	a''	$\omega(^{\circ})$	$i_L(^{\circ})$	$\Omega(^{\circ})$
A. Tokovinin, 2019	48.67	2020.76	0.867	0.428	293.6	55.1	141.1
This Study	48.98 ± 0.07	2020.799 ± 0.003	0.861 ± 0.0002	0.4250 ± 0.0005	293.95 ± 0.07	55.00 ± 0.04	140.26 ± 0.05

Table 3

The initial data for 24 Aqr.

Spectral type	F7V	(Griffin et al., 1996)
π_{Hip} (mas)	22.74 ± 0.81	(Van Leeuwen, 1997)
π_{Gaia} (mas)*	25.08 ± 0.63	(Collaboration et al., 2018)
P (days)	5.883933 ± 0.000015	(Griffin et al., 1996)
e	0.071 ± 0.006	(Griffin et al., 1996)
ω (degree)	286 ± 5	(Griffin et al., 1996)
$a \sin(i)$ (Gm)	1.178 ± 0.007	(Griffin et al., 1996)
$f(m)$ (M_{\odot})	0.00188 ± 0.00003	(Griffin et al., 1996)
T (MJD)	46988.58 ± 0.08	(Griffin et al., 1996)

(*) Gaia parallax is DR2, and that no revision was made in EDR3.

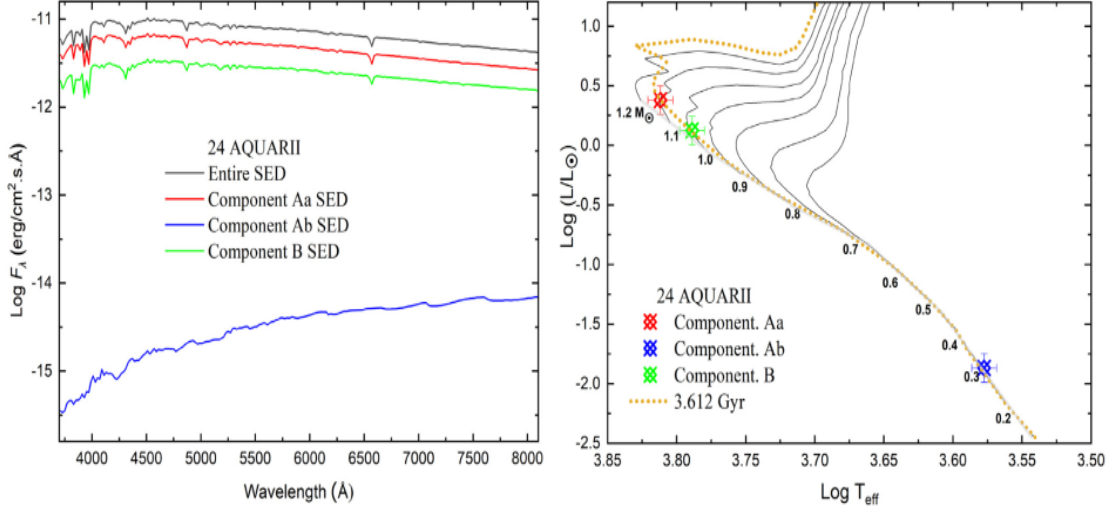


Fig. 2. The synthetic spectral energy distributions SEDs for entire and individual components for the triple system 24 Aqr using Al-Wardat's method for analyzing BMSs (left). The position of components of 24 Aqr on the HR diagram, and the evolutionary tracks (right) for solar metallicity and 3.612 Gyr isochrone. The evolutionary tracks and isochrones are taken from (Girardi et al., 2000).

Table 4
Magnitudes and color indices of the composed synthetic spectrum and individual components of 24 Aqr.

Sys.	Filter	Entire Synth.		24 Aqr		
		$\sigma = \pm 0.03$	Aa	Ab	B	
Joh-Cou.	<i>U</i>	7.21	7.54	17.94	8.69	
	<i>B</i>	7.17	7.53	16.81	8.54	
	<i>V</i>	6.66	7.08	15.11	7.90	
	<i>R</i>	6.37	6.82	14.04	7.55	
	<i>U - B</i>	0.04	0.005	1.13	0.15	
	<i>B - V</i>	0.514	0.459	1.701	0.642	
	<i>V - R</i>	0.29	0.26	1.08	0.35	
	<i>u</i>	8.38	8.72	19.49	9.84	
	<i>v</i>	7.47	7.81	17.64	8.89	
Ström.	<i>b</i>	6.95	7.34	16.39	8.26	
	<i>y</i>	6.63	7.05	15.12	7.87	
	<i>u - v</i>	0.91	0.91	1.84	0.95	
	<i>v - b</i>	0.517	0.472	1.25	0.63	
	<i>b - y</i>	0.32	0.51	1.28	0.39	
Tycho	<i>B_T</i>	7.29	7.64	17.19	8.70	
	<i>V_T</i>	6.72	7.13	15.33	7.97	
	<i>B_T - V_T</i>	0.57	0.51	1.87	0.73	

Table 5**The Fundamental parameters of the individual components of the 24 Aqr.**

Parameters	Units	24 Aqr		
		Aa	Ab	B
$T_{\text{eff}} \pm \sigma_{T_{\text{eff}}}$	[K]	6483 ± 80	3780 ± 80	6150 ± 80
$R \pm \sigma_R$	[R_{\odot}]	1.23 ± 0.04	0.28 ± 0.04	1.02 ± 0.04
$\log g \pm \sigma_{\log g}$	[cm/s^2]	4.40 ± 0.06	4.80 ± 0.06	4.47 ± 0.06
$L \pm \sigma_L$	[L_{\odot}]	2.40 ± 0.10	0.014 ± 0.09	1.33 ± 0.05
$M_{\text{bol}} \pm \sigma_{M_{\text{bol}}}$	[mag]	3.80 ± 0.08	9.42 ± 0.08	4.44 ± 0.09
$\mathcal{M} \pm \sigma_{\mathcal{M}}$	[M_{\odot}]	1.10 ± 0.09	0.29 ± 0.05	1.0 ± 0.08
Sp. Type		F5.5 V	M0.5 V	F8 V
Age	Gyr		3.612	

Table 6

Edwards' process for the inner component (A) of 24 Aqr.

Δm	S	M_{Aa}	M_{Ab}	Sp ₁	Sp ₂	$M_1(M_{\odot})$	$M_2(M_{\odot})$	$a(AU)$	$\sin(i_S)$	i_S°
1.5	0.30	3.50 ± 0.02	5.06 ± 0.01	F5V	G4V	1.20 ± 0.05	0.97 ± 0.03	0.0825 ± 0.0041	0.216	12.3 ± 0.9
4.5	0.07	3.73 ± 0.02	8.23 ± 0.02	F6V	K6V	1.17 ± 0.05	0.63 ± 0.03	0.0776 ± 0.0034	0.309	16.8 ± 1.1
6.5	0.02	3.78 ± 0.02	10.28 ± 0.02	F6V	M2V	1.16 ± 0.04	0.35 ± 0.03	0.0746 ± 0.0028	0.563	34.3 ± 2.2
8.0	0.00	3.80 ± 0.02	11.80 ± 0.05	F7V	M5V	1.14 ± 0.04	0.19 ± 0.02	0.0706 ± 0.0019	0.828	55.8 ± 2.9

Table 7

The individual masses for the components of the system 24 Aqr, along with total mass calculated using different methods.

Components	Griffin 1996	Heintz 1997	Tokovinin 2019	Visual Orbit This work	Al-Wardat method This work	Spectroscopic solution This work	Combined Solution This work
$M_{Aa}(M_{\odot})$	1.19	1.15	-	-	1.10 ± 0.09	1.14 ± 0.04	1.12 ± 0.06
$M_{Ab}(M_{\odot})$	0.15	0.15	-	-	0.29 ± 0.05	0.19 ± 0.03	0.24 ± 0.05
$M_B(M_{\odot})$	1.1	1.15	-	-	1.0 ± 0.08	1.12 ± 0.04	1.06 ± 0.05
$\Sigma M(M_{\odot})_{DR2}(25.08 \text{ mas})$	2.44	2.45	2.097	2.03	2.39	2.45 ± 0.05	2.42 ± 0.06
$\Sigma M(M_{\odot}) \pi_{H\beta 2}(22.74 \text{ mas})$		3.23	2.815	2.72	2.39		
$\Sigma M(M_{\odot}) \pi_{D_{3R}}(23.75 \text{ mas})$		3.28	2.85	2.39	2.39		

systems such as the structure and stability of the global system and explores HD196885, an extreme planetary system (Chauvin et al., 2022; Algnamat et al., 2022; Alameryeen et al., 2022). Thus, we apply the same method but for spectroscopic binaries then compare the results with any available information about physical or geometrical parameters for the visual binaries such as the total masses of the systems, the inclination, and the angular separation (q) in arc-seconds between the components (see Abushattal, 2017; Abushattal et al., 2020). This method permits the determination of the physical and geometrical properties using the available data of visual and spectroscopic binaries. It is applicable for the low-mass star with a negligible contribution in the composite spectrum. Fig. 4 is a graphical representation of the main idea this work. Starting from the visual and spectroscopic observations, it shows all steps required to calculate the physical parameters and orbital elements of the individual components and the most probable 3D orbit. The application of this method permits us to obtain the spectrum of each component from the composite spectrum of the system. We use the following equations (Edwards, 1976; Abushattal, 2017; Abushattal et al., 2020):

$$M(S_1) + x M(S_2) = (1 + x) M(S_{1+2}) \quad (4)$$

where $M(S_1)$, $M(S_2)$, $M(S_{1+2})$ are the absolute magnitudes. $(S_{1,2})$ is the absolute magnitude and the visual magnitude difference by :

$$\Delta m = M(S_2) - M(S_1) = M_2 - M_1 = -2.5 \log(x) \quad (5)$$

Then Edwards equations can be expressed in the form:

$$M_1 + xM_2 = (1 + x)M \quad (6)$$

then we deduce

$$M_1 = M - \frac{x\Delta m}{1 + x}. \quad (7)$$

This expression relates (M_1) the absolute magnitude of the first component with (M) the total absolute magnitude by means of a step, S . In this work the global absolute magnitude (M) based on the apparent magnitude and the parallax of the system using well-known relation:

$$M = m + 5 + 5 \log(\pi). \quad (8)$$

Therefore, we can represent Edwards step (S) as a function of Δm for Single-lined (SB1) and double-lined (SB2) spectroscopic binaries:

$$S = \frac{x \cdot \Delta m}{1 + x}. \quad (9)$$

Then the composite spectrum is evaluated and so, for each value of Δm , we can calculate the value of S in Table 6 and then, using the following relation we can calculate the absolute magnitudes of the both components of the system:

$$M_1 = M - S, \quad M_2 = M_1 + \Delta m. \quad (10)$$

The spectral types, the masses and the errors for each of them can be determined using the calibrations in (Abushattal et al., 2020 and Pecaut and Mamajek, 2013). Then we use the value of the mass function from the spectroscopic orbital solution and substitute the previous masses in the following relation in order to determine the inclination (i_S) of the system (see Table 6):

$$i_S = \sin^{-1} \left(\frac{\sqrt[3]{f(M)(M_1 + M_2)^2}}{M_2} \right) \quad (11)$$

Therefore, using data from Table 3 we analyzed the spectroscopic component (A) in this triple system in order to describe the physical parameters for Aa and Ab and compare them with those previously published. So, depending on the value of the Gaia parallax (Collaboration et al., 2018), the Edwards process in this work, and the radial velocity information the most probable value of the masses of 24 Aqr are as follows: the mass of the first component (A) is $M_A = 1.36 \pm 0.05 M_\odot$ with $M_{Aa} = 1.14 \pm 0.04 M_\odot$ and $M_{Ab} = 0.19 \pm 0.02 M_\odot$, while the mass of the second component (B) is $M_B = 1.12 \pm 0.03 M_\odot$. Hence, the total mass of the system is $M_t = 2.45 \pm 0.05 M_\odot$ (see Table 7).

We employed both the Al-Wardat and Edwards methods, which are observation-based and thus yielded varying results. Consequently, we opted for the average value listed at the table's end. This average value provides a central measure for the masses, offering simplicity and comparability.

3 Orbital alignment

The system is a hierarchical triple system with well-separated components since the orbital period of the visual binary is more than 3000 times larger than the one of the spectroscopic pair. A triple system with such a large period ratio is dynamically very stable (e.g. Georgakarakos, 2013). The mutual inclination between the orbital planes of motion in multistellar systems is an important parameter in order to understand the system's formation and evolution (e.g. Sterzik and Tokovinin, 2002; Tokovinin, 1997; Tokovinin, 2014b).

The mutual inclination I between two orbits can be found by (e.g. Fekel, 1981; Docobo, 1977)

$$\cos(I) = \cos(i_L) \cos(i_S) + \sin(i_L) \sin(i_S) \cos(\Omega_L - \Omega_S), \quad (12)$$

where i_L and i_S are the orbital inclinations for the outer (L) and inner (S) orbit respectively, and Ω_L and Ω_S are the corresponding ascending node longitudes. The spectroscopic binary has $i_S = 55.8^\circ$, while we have found for the visual binary that $i_L = 55.0^\circ$ and $\Omega_L = 140.26^\circ$. Since the longitude of the ascending node of the inner orbit Ω_S is unknown, the mutual inclination between the two orbits cannot be determined; but it falls within the range

$$55.8^\circ - 55.0^\circ \leq I \leq 55.8^\circ + 55.0^\circ \Rightarrow 0.8^\circ \leq I \leq 110.8^\circ, \quad (13)$$

or

$$124.2^\circ - 55.0^\circ \leq I \leq 124.2^\circ + 55.0^\circ \Rightarrow 69.2^\circ \leq I \leq 179.2^\circ \quad (14)$$

if we consider a retrograde orbit for the spectroscopic binary. The orbital configuration along with the masses of the stars, however, may provide us with some clues so that we can further constrain the mutual inclination value. Our system consists of a close inner binary with a period of about 5.8 days and a mass ratio $m_2 = m_1$ around 0.21 and a third star at 17.97 au on an elliptic orbit of 0.861 eccentricity. Generally, the formation of close binaries is a complex problem with many pending questions (Kratter, 2011), involving different formation channels (Bate et al., 2002). The formation history of a triple system can provide information regarding the orientation of the orbital planes of the system. According to Bate (2009), the formation of a triple system from disc fragmentation around an initially single object or a flatten core, favours aligned orbital planes. In addition, the accretion of mass in a triple system that forms with initially non-coplanar orbital planes may result in a decrease of the mutual inclination of that system into closer alignment. Finally, triple systems formed from single object capture by a binary may have their orbital planes very misaligned. A passing object can have a similar effect on the alignment of the orbital planes of a triple system.

One possible mechanism of producing short period binaries in hierarchical triple systems is Kozai cycles with tidal friction (KCTF) (e.g. Fabrycky and Tremaine, 2007). As noticed by Kozai (1962)

and Lidov (1962), a highly inclined ($39.2^\circ < I < 140.8^\circ$) tertiary companion with respect to the orbital plane of a binary orbit would push the eccentricity of the binary to high values, even to 1 for a perpendicular configuration. As the high eccentricity values lead to close pericentre passages for the two members of the inner binary, tidal friction becomes important and works towards the shrinking and circularisation of the binary orbit. Other effects, such as for example the relativistic precession of the pericentre of the binary orbit, are also expected to contribute to the orbital evolution of the system. In their numerical experiments, Fabrycky and Tremaine (2007) found that KCTF produced triple systems with very large period ratios, circular inner orbits, and a mutual inclination that was often near the critical one. Moe and Kratter (2018), however, suggested that only a fraction of close binaries can be explained through the KCTF mechanism. They also stated that 60% of close binaries with orbital periods less than 10 days derive from the dynamical unfolding of initially unstable triples that fragment in the disk coupled with significant energy dissipation within the disk. The close binaries formed that way have almost coplanar tertiary components in configurations where the outer semi-major axis is between 0.5 and 50 au. This formation channel operates exclusively during the pre-MS phase while there is still dissipative gas in the primordial disk. Hence, interactions of coplanar triples embedded in disks, not secular evolution of misaligned triples nor disk migration of solitary binaries, may explain the majority of very close binaries. Similar formation scenarios are discussed in Tokovinin (2020) and Tokovinin and Moe (2020).

Moreover, Bate (2012); Bate (2014), after performing hydrodynamical simulations of star cluster formation, concluded that both observed and simulated triple systems have a tendency towards orbital coplanarity. This conclusion seems to be supported by Tokovinin (2017), where he found a rather strong tendency of orbit alignment in triple stars where the outer separation was less than 50 au. He also found that the orbit alignment was stronger in triple stars with low-mass primaries. It is also, however, pointed out in that work that gas accretion by the stars can create misaligned triples in systems with randomly aligned angular momentum at the epoch of star formation. Along with changes in the outer orbit orientation, it can also cause the rapid inward migration of the outer body. This may increase the intensity of the gravitational perturbations among the bodies of the system, which in certain cases may even lead to its destabilization. Such kind of dynamical interactions in multi-body systems could result in misaligned triples and often with highly eccentric orbits (Antognini and Thompson, 2016). On the other hand, triple stars produced in N-body decay, with or without accretion, usually have moderate period ratios (≈ 10) and outer mass ratios $m_3/(m_1 + m_2) < 0.2$ (Tokovinin, 2008).

Griffin et al. (1996) gave a 0.071 eccentricity for the spectroscopic binary orbit. Assuming coplanar orbits, from the work of Georgakarakos (2003), the forced eccentricity of the spectroscopic binary orbit is

$$e_{forced} = \frac{C}{B - A} \approx 0.0150, \quad (15)$$

where

$$\begin{aligned} A &= \frac{\mathcal{M}_{Aa}\mathcal{M}_{Ab}\mathcal{M}_t^{1/2}}{\mathcal{M}_B\mathcal{M}_A^{3/2}} \left(\frac{a_S}{a_L} \right)^{1/2} \frac{1}{(1 - e_L^2)^2} \\ B &= \frac{1}{(1 - e_L^2)^{3/2}} + \frac{25}{8} \frac{\mathcal{M}_B}{\mathcal{M}_t^{1/2}\mathcal{M}_A^{1/2}} \left(\frac{a_S}{a_L} \right)^{3/2} \frac{3 + 2e_L^2}{(1 - e_L^2)^3} \\ C &= \frac{5}{4} \frac{\mathcal{M}_{Aa} - \mathcal{M}_{Ab}}{\mathcal{M}_A} \frac{a_S}{a_L} \frac{e_L}{(1 - e_L^2)^{5/2}}, \end{aligned}$$

with $\mathcal{M}_{Aa} = 1.12\mathcal{M}_\odot$, $\mathcal{M}_{Ab} = 0.24\mathcal{M}_\odot$, $\mathcal{M}_B = 1.06\mathcal{M}_\odot$, $a_S = 0.0706au$, $a_L = 17.97au$ and $e_L = 0.861$.

If the spectroscopic orbit is initially circular, its maximum orbital eccentricity will reach the value of 0.030, i.e. twice the value of the forced eccentricity but still well below our current 0.071. Of course, that maximum value can be higher if we consider that the initial eccentricity of the spectroscopic binary is not zero. Considering a mutually inclined orbit could easily provide the value we observe as long as $i > 39.2^\circ$. We have to point out here that since the semi-major axis of the inner binary is 0.0706 au, other effects, such as tidal friction, deformation of the shape of the stars due to rotation, and general relativity may contribute to the evolution of the inner orbit by suppressing Kozai cycles (Fabrycky and Tremaine, 2007; Taani et al., 2020). But even at low mutual inclinations or coplanar orbits the result will be the same, i.e. the eccentricity oscillations will be suppressed resulting in lower amplitudes. Fig. 3 demonstrates that effect for different values of the mutual inclination i . In those plots, we have only taken into consideration the general relativistic effect which, based on some crude estimates using the equations given in Fabrycky and Tremaine (2007), seems to be the dominant one here. A quick calculation yields an order of magnitude of 10^{-4} for the rate of the relativistic pericentre precession, while the precession rate due to tidal distortion is an order of magnitude less, i.e. 10^{-5} . Finally, the precession rate due to the rotational distortion of the stars is several orders of magnitude smaller than the other two effects. Only in the case of a highly inclined outer orbit we can achieve the value of the eccentricity of the spectroscopic orbit as given in Griffin et al. (1996). More specifically, taking into consideration general relativistic effects, the mutual inclination of the system needs to be above 60° and less than 120° if we want to achieve a spectroscopic binary eccentricity of about 0.071.

To summarise, the mutual inclination of the system seems to be in the range $[0.8^\circ, 110.8^\circ]$ or $[69.2^\circ, 179.2^\circ]$ i.e. the system could be nearly coplanar, highly inclined or having the distant star to move on a retrograde orbit with respect to the spectroscopic binary. There are certain characteristics regarding the orbits and masses of the system that may point towards the alignment or not of the two orbital planes. On the other hand, it appears that the observed value of 0.071 for the eccentricity of the spectroscopic binary is easier to be achieved by Kozai-Lidov oscillations, even though they are suppressed by other physical processes.

4 Is it possible to resolve this system visually?

In 2021, the wide system passed through the periastron passage, which helped us determine the dips, rotational velocities, and mass ratios of the system's components. A valid question to answer is whether it is possible to resolve the entire 24 Aqr system visually. In other words, what is the size of the telescope we need to resolve the inner system? Previously, we determined the physical and orbital elements of the entire system. We have all the required parameters to calculate the ephemerides of the inner spectroscopic binary by the algorithm for visual binaries. We only need to describe the position of the inner binary components in the apparent plane where the polar coordinates θ and ρ are defined. We will measure the position angle θ from the line of the nodes. Then we can describe the relative orbit based on two-body formulae and we determine the coordinates r and f for an epoch t . We calculate the separation between the components of the inner binary by estimating the mean anomaly, l , then calculate the eccentric anomaly, E , using the following equation from (Abushattal, 2017; Abushattal et al., 2020):

$$r'' = a'' (1 - e \cos (E)) \quad (16)$$

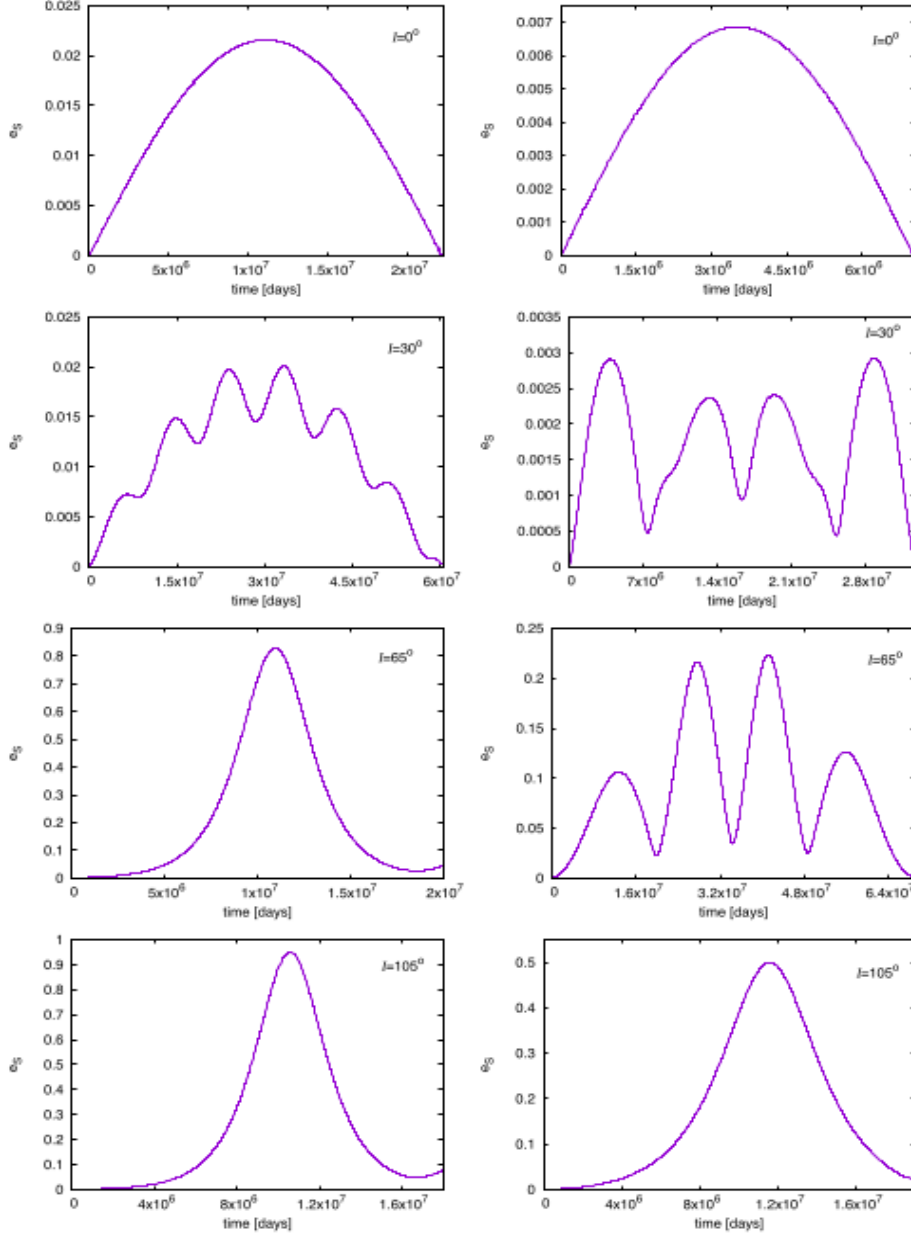


Fig. 3. Spectroscopic binary eccentricity against time for various values of the mutual inclination I . The left column plots come from the numerical integration of the full equations of motion of the system (Newtonian gravity only). The right column plots come from the numerical integration of the Einstein-Infeld-Hoffmann equations. Note the differences in the period and amplitude of the oscillations between the plots of the left and right column. The plots were generated using a Gauss-Radau scheme (Eggel and Dvorak, 2010).

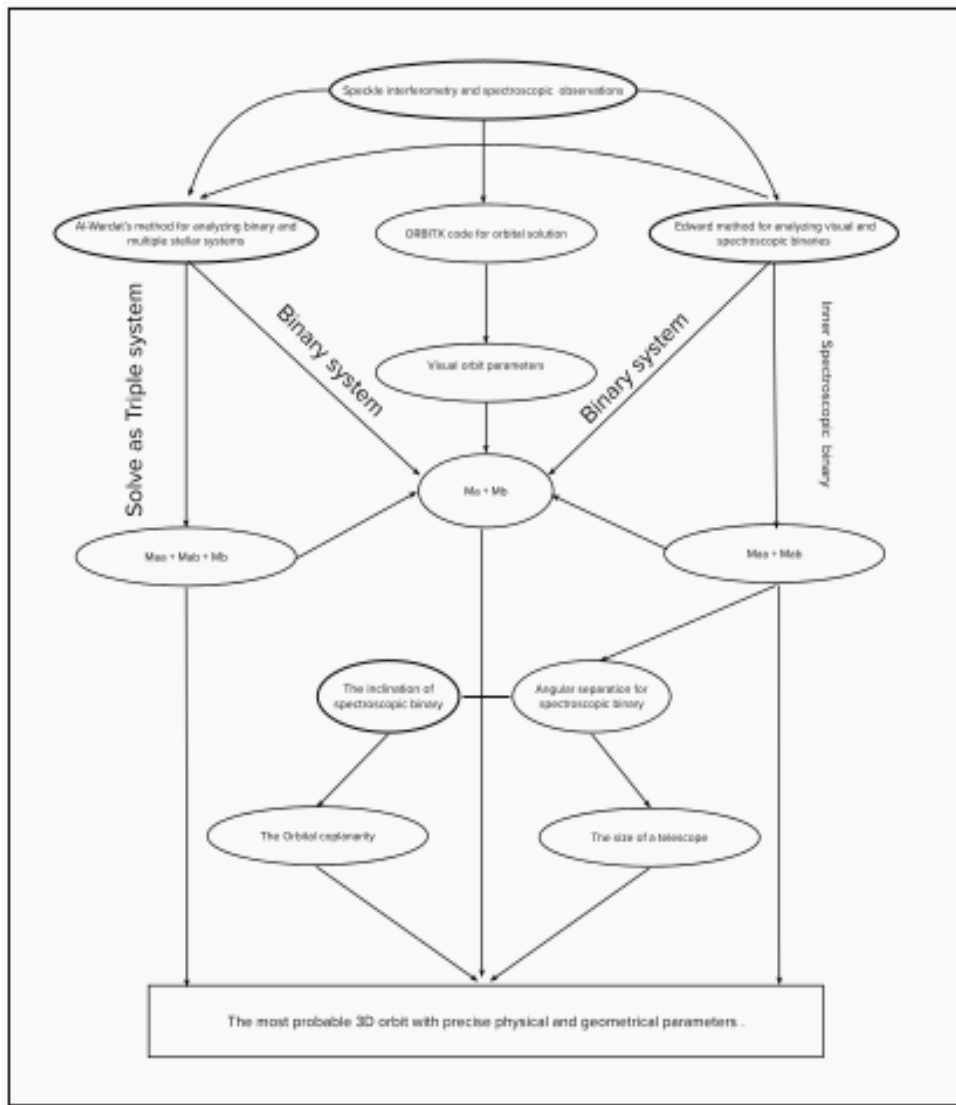


Fig. 4. A flowchart of the methodology used in the analysis of triple system 24 Aqr.

where the double prime denotes arcsecs, and the true anomaly,

$$\tan\left(\frac{f}{2}\right) = \sqrt{\frac{1+e}{1-e}} \tan\left(\frac{E}{2}\right). \quad (17)$$

Then

$$\tan(\theta - \Omega) = \tan(\omega + f) \cos i \quad (18)$$

and

$$\rho'' = r'' \frac{\cos(\omega + f)}{\cos(\theta - \Omega)}. \quad (19)$$

ω is the longitude of the periastron, and we assume that $\Omega = 0^\circ$. Then we can calculate θ and ρ'' . More details about the above calculations can be found in Abushattal et al. (2020). The apparent orbit can be drawn sufficiently using $0^\circ \leq \theta \leq 360^\circ$ in (18). f can be calculated using same expression (18). Then we can describe the minimum and maximum separation ρ between the components of the inner orbit.

The ability of the telescope to resolve the binary stars visually depends on many factors such as relative brightness, lens and mirror coatings, the condition of sky, and light pollution even the observer experience. “The Double Double” star, also known as Epsilon Lyrae in the constellation of Lyra, is an example for the relation between the power separation between the components and the increase of the size of the telescopes; Dawes limit describes that with the following formula (Mullaney, 2006):

$$D = \frac{11.7}{\rho''}, \quad (20)$$

where the angular separation ρ is in arc seconds and the diameter D in centimeters. Hence, we use the maximum value for ρ derived by the equations above and which equals to $0.0018''$. In this case, we need a telescope with a diameter larger than 65 meters to resolve the inner spectroscopic binary in 24 AQUARI triple system. We suggest that the system should be observe with a large array of telescopes such as CHARA (Center for High Angular Resolution Astronomy) array and Navy Precision Optical Interferometer (NPOI) which have resolving capability larger than 300 meters as single telescope. Also, we can put this system as a test for future high resolution monitoring tools.

5 Conclusions

We present a spectro-interferometric analysis, atmospheric modeling and synthetic photometry for the hierarchical triple System 24 Aqr. We used new relative position measurements to modify the orbit of the outer system and to find new orbital elements and dynamical parallax. Three different methods were used in the analysis, these are: Tokovinin’s dynamical method (ORBITX) for calculating the orbit of the outer binary. Edwards’ method for solving the inner single-line spectroscopic binary. Al-Wardat’s method for analyzing binary and multiple stellar systems for building synthetic SEDs for each of the three components, and for estimating the complete set of physical and geometrical parameters of the system, including individual masses, synthetic photometry and a new parallax for the system. The main conclusions of this work can be summarized as follows:

- A modified orbital solution, and new orbital elements were calculated for the outer binary using four new speckle-interferometric measurements.

- We estimated the individual masses of the system using a combination of different methods. Edwards' method gives $\mathcal{M}_{Aa} = 1.14 \pm 0.04 \mathcal{M}_\odot$ and $\mathcal{M}_{Ab} = 0.19 \pm 0.03 \mathcal{M}_\odot$ and $\mathcal{M}_B = 1.12 \pm 0.04 \mathcal{M}_\odot$. Al-Wardat's method gives $\mathcal{M}_{Aa} = 1.10 \pm 0.09 \mathcal{M}_\odot$ and $\mathcal{M}_{Ab} = 0.29 \pm 0.05 \mathcal{M}_\odot$ and $\mathcal{M}_B = 1.0 \pm 0.08 \mathcal{M}_\odot$.
- We introduced accurate atmospheric and fundamental parameters for the individual components. These parameters include the individual masses, the effective temperatures, gravity, stellar radii, luminosity, magnitudes, color indices, spectral types and ages.
- According to Al-Wardat's method, which barely affected by any change in the parallax measurements, as it is clear in Table 7, and as it was concluded by Al-Wardat et al. (2021b), the best estimation for the mass sum of the system is $(2.74 \pm 0.18 \mathcal{M}_\odot)$. This leads us to adopt a new dynamical parallax for the system as $\pi_{Dyn}(\pi = 22.63 \pm 0.25 \text{ mas})$, which is very close to that given by Hipparcos 2 as $22.74 \pm 0.81 \text{ mas}$. DR2 has an atypically large error, DR3 has no parallax update and neither resolves the components, and we will have to wait to see about DR4. Thus, our dynamical parallax is in fact the most precise value that exists at present, it is one of the unique aspects of our analysis.
- We discussed the orbital alignment of the two orbits in this hierarchical stellar triple.
- Finally, we gave the required specifications of the telescope to resolve the inner spectroscopic system interferometrically.

Data availability

We will publish the new measurements used in this calculation in this article. The stellar data and other measurements were obtained from the data bases and catalogs mentioned in the acknowledgments. In response to reasonable requests, the corresponding author will provide the data underlying this article.

Declaration of Competing Interest

The authors declare that they have no known competing financial interests or personal relationships that could have appeared to influence the work reported in this paper.

Acknowledgments

Thank Gerard van Belle, Catherine Clarck, and Zachary Hartman at Lowell Observatory for helping us obtain the QWSSI observations. We are grateful to US Naval Observatory for both the Fourth Catalog of Interferometric Observations of Binary Stars and the Washington Double Star Catalog. Also, to Centre de donnees astronomiques de Strasbourg (CDS), Strasbourg, France for the available SIMBAD database. This work has made use of data from the European Space Agency (ESA) mission Gaia(<https://www.cosmos.esa.int/gaia>), processed by the Gaia Data Processing and Analysis Consortium (DPAC, <https://www.cosmos.esa.int/web/gaia/dpac/consortium>). It also has made use of SIMBAD database, the Fourth Catalog of Interferometric Measurements of Binary Stars, IPAC datasystems, and codes of Al-Wardat's method for analyzing binary and multiple stellar systems.

References

Abt, H., 1985. Visual multiples. viii-1000 mk types. *Astrophys. J. Suppl. Ser.* 59, 95–112.

Abu-Alrob, E.M., Hussein, A.M., Al-Wardat, M.A., 2023. Atmospheric and fundamental parameters of the individual components of multiple stellar systems. *Astronom. J.* 165 (6), 221. <https://doi.org/10.3847/1538-3881/acc9ab>.

Abushattal, A., Al-Wardat, M., Taani, A., Khassawneh, A., Al-Naimiy, H., 2019. Extrasolar planets in binary systems (statistical analysis). *Journal of Physics: Conference Series*, vol. 1258. IOP Publishing, p. 012018.

Abushattal, A., Alrawashdeh, A., Kraishan, A., 2022a. Astroinformatics: The importance of mining astronomical data in binary stars catalogues. *Commun. BAO* 69 (2), 251–255.

Abushattal, A., Kraishan, A., Alshamaseen, O., 2022b. The exoplanets catalogues and archives: An astrostatistical analysis. *Commun. BAO* 69 (2), 235–241.

Abushattal, A.A., 2017. The modeling of the physical and dynamical properties of spectroscopic binaries with an orbit: doctoral dissertation. Universidade de Santiago de Compostela, Ph.D. thesis.

Abushattal, A.A., Docobo, J.A., Campo, P.P., 2020. The most probable 3D Orbit for spectroscopic binaries. *Astronom. J.* 159 (1), 28. <https://doi.org/10.3847/1538-3881/ab580a>.

Aitken, R., Millard, R.E., 1932. The orbit of the binary system b1212= 24 aquarii. *Publ. Astron. Soc. Pac.* 44 (258), 129–131.

Aitken, R.G., 1932. The Orbit of the binary system b 1212=24. Aquarii. 44 (258), 129. <https://doi.org/10.1086/124215>.

Al-Tawalbeh, Y.M., Hussein, A.M., Taani, A., Abushattal, A., Yusuf, N., Mardini, M., Suleiman, F., Al-Naimiy, H.M., Khasawneh, A.M., Al-Wardat, M.A., 2021. Precise masses, ages, and orbital parameters of the binary systems hip 11352, hip 70973, and hip 72479. *Astrophys. Bull.* 76, 71–83.

Al-Wardat, M., 2012. Physical parameters of the visually close binary systems Hip70973 and Hip72479. *Publ. Astronom. Soc. Aust.* 29 (4), 523–528. <https://doi.org/10.1071/AS12004>, arXiv:1204.4589.

Al-Wardat, M., Docobo, J., Abushattal, A., Campo, P., 2017. Physical and geometrical parameters of cvbs. xii. fin 350 (hip 64838). *Astrophys. Bull.* 72(1), 24–34.

Al-Wardat, M.A., 2002. Spectral energy distributions and model atmosphere parameters of the quadruple system ADS11061. *Bull. Special Astrophys. Obser.* 53, 51–57.

Al-Wardat, M.A., 2003a. Model atmosphere parameters of the binary system 41 Dra. *Bull. Special Astrophys. Obser.* 56, 41–45.

Al-Wardat, M.A., 2003b. Spectral energy distributions and model atmosphere parameters of the binary systems COU1289 and COU1291. *Bull. Special Astrophys. Obser.* 56, 36–40.

Al-Wardat, M.A., 2007. Model atmosphere parameters of the binary systems COU1289 and COU1291. *Astron. Nachr.* 328 (1), 63–67. <https://doi.org/10.1002/asna.200610676>.

Al-Wardat, M.A., 2008. Synthetic photometry of speckle interferometric binaries. *Astrophys. Bull.* 63 (4), 361–365. <https://doi.org/10.1134/S1990341308040044>.

Al-Wardat, M.A., Abu-Alrob, E., Hussein, A.M., Mardini, M.K., Taani, A.A., Widyan, H.S., Yousef, Z.T., Al-Naimiy, H.M., Yusuf, N.A., 2021a. Physical and geometrical parameters of CVBS XIV: the two nearby systems HIP 19206 and HIP 84425. *Res. Astron. Astrophys.* 21 (7), 161. <https://doi.org/10.1088/1674-4527/21/7/161>, arXiv:2111.11675.

Al-Wardat, M.A., Hussein, A.M., Al-Naimiy, H.M., Barstow, M.A., 2021b. Comparison of Gaia and Hipparcos parallaxes of close visual binary stars and the impact on determinations of their masses. *Publ. Astronom. Soc. Aust.* 38, e002. <https://doi.org/10.1017/pasa.2020.50>, arXiv:2111.05325.

Al-Wardat, M.A., Widyan, H., 2009. Parameters of the visually close binary system Hip11253

(HD14874). *Astrophys. Bull.* 64 (4), 365–371. <https://doi.org/10.1134/S1990341309040063>.

Al-Wardat, M.A., Widyan, H.S., Al-thyabat, A., 2014. Complex analysis of the stellar binary HD25811: a subgiant system. *Publ. Astronom. Soc. Aust.* 31, e005. <https://doi.org/10.1017/pasa.2013.42>, arXiv:1311.5721.

Alameryeen, H., Abushattal, A., Kraishan, A., 2022. The physical parameters, stability, and habitability of some double-lined spectroscopic binaries. *Commun. BAO* 69 (2), 242–250.

Algnamat, B., Abushattal, A., Kraishan, A., Alnaimat, M., 2022. The precise individual masses and theoretical stability and habitability of some single-lined spectroscopic binaries. *Commun. BAO* 69 (2), 223–230.

Anguita-Aguero, J., Mendez, R.A., Claveria, R.M., Costa, E., 2022. Orbital elements and individual component masses from joint spectroscopic and astrometric data of double-line spectroscopic binaries. *Astron. J.* 163 (3), 118.

Antognini, J.M.O., Thompson, T.A., 2016. Dynamical formation and scattering of hierarchical triples: cross-sections. *Kozai-Lidov Oscillations Collisions.* 456 (4), 4219–4246. <https://doi.org/10.1093/mnras/stv2938>, arXiv:1507.03593.

Balega, Y.Y., Ryadchenko, V., 1984. Digital speckle interferometry of binary stars. *Soviet Astron. Lett.* 10, 95–98.

Bate, M.R., 2009. Stellar, brown dwarf and multiple star properties from hydrodynamical simulations of star cluster formation., 392(2), 590–616. <https://doi.org/10.1111/j.1365-2966.2008.14106.x>, arXiv:0811.0163.

Bate, M.R., 2012. Stellar, brown dwarf and multiple star properties from a radiation hydrodynamical simulation of star cluster formation. 419(4), 3115–3146. <https://doi.org/10.1111/j.1365-2966.2011.19955.x>, arXiv:1110.1092.

Bate, M.R., 2014. The statistical properties of stars and their dependence on metallicity: the effects of opacity. 442(1), 285–313. <https://doi.org/10.1093/mnras/stu795>, arXiv:1405.5583.

Bate, M.R., Bonnell, I.A., Bromm, V., 2002. The formation of close binary systems by dynamical interactions and orbital decay. 336(3), 705–713. <https://doi.org/10.1046/j.1365-8711.2002.05775.x>, arXiv:astro-ph/0212403.

Blaauw, A., Strand, K.A., 1963. Basic astronomical data. *Aa. Strand*, Ed, p. 383.

Bonneau, D., Blazit, A., Foy, R., Labeyrie, A., 1980. Speckle interferometric measurements of binary stars. *Astron. Astrophys. Suppl. Ser.* 42, 185–188.

Cannon, A., Pickering, E., 1924. Henry draper (hd) catalog and hd extension. *hdhc*.

Carter, J.A., Fabrycky, D.C., Ragozzine, D., Holman, M.J., Quinn, S.N., Latham, D.W., Buchhave, L.A., Van Cleve, J., Cochran, W.D., Cote, M.T., et al., 2011. Koi-126: A triply eclipsing hierarchical triple with two low-mass stars. *Science* 331 (6017), 562–565.

Chauvin, G., Videla, M., Beust, H., Mendez, R., Correia, A., Lacour, S., Tokovinin, A., Hagelberg, J., Bouchy, F., Boisse, I. et al., 2022. Chasing extreme planetary architectures: I-hd196885ab, a super-jupiter dancing with two stars? arXiv preprint arXiv:2211.00994.

Christy, J.W., Walker Jr, R., 1969. Mk classification of 142 visual binaries. *Publications of the Astronomical Society of the Pacific*, pp. 643–649.

Clark, C.A., Van Belle, G.T., Horch, E.P., Trilling, D.E., Hartman, Z.D., Collins, M., Von Braun, K., Gehring, J., 2020. The optomechanical design of the quad-camera wavefront-sensing six-channel speckle interferometer (qwssi). In: *Optical and Infrared Interferometry and Imaging VII*, vol. 11446, SPIE, pp. 540–548.

Collaboration, G. et al., 2018. Vizier online data catalog: Gaia dr2 (gaia collaboration, 2018). *yCat*, pp. I–345.

Danjon, A., 1942. Orbites de 24 aquarii, a 88 et beta 612. *J. des Obser.* 25, 18.

Derekas, A., Kiss, L.L., Borkovits, T., Huber, D., Lehmann, H., Southworth, J., Bedding, T.R.,

Balam, D., Hartmann, M., Hrudkova, M., et al., 2011. Hd 181068: A red giant in a triply eclipsing compact hierarchical triple system. *Science* 332 (6026), 216–218.

Docobo, J., Balega, Y., Campo, P., Abushattal, A., 2018a. Double stars inf.

Docobo, J., Campo, P., Abushattal, A., 2018b. Iau commiss. Double Stars 169, 1.

Docobo, J.A., Andrade, M., 2006. A methodology for the description of multiple stellar systems with spectroscopic subcomponents. *Astrophys. J.* 652 (1), 681.

Docobo, J.A., Griffin, R.F., Campo, P.P., Abushattal, A.A., 2017. Precise orbital elements, masses and parallax of the spectroscopic-interferometric binary hd 26441. *Mon. Not. R. Astron. Soc.* 469 (1), 1096–1100.

Edwards, T., 1976. Mk classification for visual binary components. *Astron. J.* 81, 245–249.

Eggen, O.J., 1963. The empirical mass-luminosity relation. *Astrophys. J. Suppl. Ser.* 8, 125.

Eggl, S., Dvorak, R., 2010. An introduction to common numerical integration codes used in dynamical astronomy. In: Souchay, J., Dvorak, R.(Eds.), *Lecture Notes in Physics*, vol. 790, Berlin Springer Verlag, https://doi.org/10.1007/978-3-642-04458-8_9, pp. 431–480.

Fabrycky, D., Tremaine, S., 2007. Shrinking binary and planetary orbits by kozai cycles with tidal friction. *Astrophys. J.* 669 (2), 1298.

Fekel, F.C., Scarfe, C., Barlow, D., Duquennoy, A., McAlister, H.A., Hartkopf, W., Mason, B., Tokovinin, A., 1997. New and improved parameters of hd 202908= ads 14839: a spectroscopic-visual triple system. *Astron. J.* 113, 1095.

Fekel Jr, F., 1981. The properties of close multiple stars. *Astrophys. J.* 246, 879–898.

Finsen, W., 1929a. The orbit of 24 aquarii (beta 1212, bu. gc 11125). 23h 34m 4,-0 30'(1900). *Circ. Union Obser. Johannesburg* 81, 112–114.

Finsen, W.S., 1929b. The Orbit of 24 Aquarii (b 1212, Bu. G.C. 11125). 23h 34m4, -0 30' (1900). *Circ. Union Obser. Johannesburg* 81, 112– 114.

Gaspar, A., Rieke, G.H., Ballering, N., 2016. The correlation between metallicity and debris disk mass. *Astrophys. J.* 826 (2), 171. <https://doi.org/10.3847/0004-637X/826/2/171>, arXiv:1604.07403.

Georgakarakos, N., 2002. Eccentricity generation in hierarchical triple systems with coplanar and initially circular orbits. *Mon. Not. R. Astron. Soc.* 337 (2), 559–566.

Georgakarakos, N., 2003. Eccentricity evolution in hierarchical triple systems with eccentric outer binaries. 345(1), 340–348. <https://doi.org/10.1046/j.1365-8711.2003.06942.x>. arXiv:1408.5890.

Georgakarakos, N., 2005. Erratum: Eccentricity evolution in hierarchical triple systems with eccentric outer binaries. *Mon. Not. R. Astron. Soc.* 362 (2), 748–748.

Georgakarakos, N., 2013. The dependence of the stability of hierarchical triple systems on the orbital inclination. 23, 41–48. <https://doi.org/10.1016/j.newast.2013.02.004>. arXiv:1302.5599.

Girardi, L., Bressan, A., Bertelli, G., Chiosi, C., 2000. Evolutionary tracks and isochrones for low -and intermediate- mass stars: From 0.15 to 7 Msun, and from Z=0.0004 to 0.03. *Astronom. Astrophys. Suppl. Ser.* 141, 371–383. <https://doi.org/10.1051/aas:2000126>, arXiv:astro-ph/ 9910164.

Girardi, L., Bressan, A., Bertelli, G., Chiosi, C., 2000. Vizier online data catalog: Low-mass stars evolutionary tracks and isochrones (girardi+, 2000). *VizieR Online Data Catalog*, pp. J-A+.

Griffin, R., Carquillat, J., Ginestet, N., Udry, S., 1996. Spectroscopic binary orbits from photoelectric radial velocities. paper 128: 24 aquarii. *Observatory* 116, 162–175.

Harlan, E., 1974. Mk classification for f-and g-type stars. iii. *Astron. J.* 79, 682–686.

Hartkopf, W., Mason, B., Wycoff, G., McAlister, H., 2010. Fourth catalogue of interferometric measurements of binary stars, [http://ad.usno.navy.mil/wds/int4.html\(ic4\)](http://ad.usno.navy.mil/wds/int4.html(ic4)).

Heintz, W., 1981. Radial velocities of binary and proper-motion stars. *Astrophys. J. Suppl. Ser.* 46, 247.

Heintz, W.D., 1997. The triple star 24 aquarii. *Observatory* 117, 93–93. Hussein, A.M., Abu-Alrob, E.M., Mardini, M.K., Alslaihat, M.J., Al-Wardat, M.A., 2023. Complete analysis of the subgiant

stellar system: Hip 102029. *Adv. Space Res.*

Hussein, A.M., Al-Wardat, M.A., Abushattal, A., Widyan, H.S., Abu- Alrob, E.M., Malkov, O., Barstow, M.A., 2022. Atmospheric and fundamental parameters of eight nearby multiple stars. *Astronom. J.* 163 (4), 182. <https://doi.org/10.3847/1538-3881/ac4fc7>.

JA Docobo, D., 1977. Aplicacion de la teoria de perturbaciones al estudio de sistemas estelares triples. Ph.D. thesis Universidad de Zaragoza.

Kozai, Y., 1962. Secular perturbations of asteroids with high inclination and eccentricity. *Astronom. J.* 67, 591–598. <https://doi.org/10.1086/108790>.

Kratter, K.M., 2011. The Formation of Close Binaries. In: Schmidtobre- ick, L., Schreiber, M.R., Tappert, C. (Eds.), *Evolution of Compact Binaries*, vol. 447, Astronomical Society of the Pacific Conference Series, p. 47. arXiv:1109.3740.

Kuiper, G., 1926. The orbit of bu. gc 11125= beta1212= 24 aquarii. *Bull. Astron. Inst. Netherlands* 3, 147.

Kurucz, R., 1994a. Atomic Data for Ca, Sc, Ti, V, and Cr. *Atomic Data for Ca*, 20.

Kurucz, R., 1994b. Atomic Data for Fe and Ni. *Atomic Data for Fe and Ni*. Kurucz CD-ROM No. 22. Cambridge, 22.

Kurucz, R., 1994c. Atomic Data for Mn and Co., Atomic Data for Mn and Co. Kurucz CD-ROM No. 21. Cambridge, 21.

Kurucz, R., 1994d. Solar abundance model atmospheres for 0,1,2,4,8 km / s. Solar abundance model atmospheres for 0, 19.

Kurucz, R.L., 1994e. Computation of Opacities for Diatomic Molecules. In: Jorgensen, U.G. (Ed.), *IAU Colloq. 146: Molecules in the Stellar Environment*, vol. 428. p. 282, <https://doi.org/10.1007/3-540-57747-5.51>.

Lidov, M.L., 1962. The evolution of orbits of artificial satellites of planets under the action of gravitational perturbations of external bodies. 9 (10), 719–759. [https://doi.org/10.1016/0032-0633\(62\)90129-0](https://doi.org/10.1016/0032-0633(62)90129-0).

Lippincott, S., 1982. Masses mass ratios and parallaxes from astrometric studies of seven visual binaries. *Astron. J.* 87, 1237.

Malkov, O.Y., 2007. Mass–luminosity relation of intermediate-mass stars. *Mon. Not. R. Astron. Soc.* 382 (3), 1073–1086.

Mannino, G., 1946. Orbita provvisoria delle doppie visuali ADS 15176 = 24 Aquarii ed ADS 15267 = H0 166, 18, 133.

Mannino, G., Humblet, J., 1955. Observations spectroscopiques de quelques étoiles of (i). In: *Annales d'Astrophysique*, vol. 18, p. 237.

Masda, S.G., Docobo, J.A., Hussein, A.M., Mardini, M.K., Al-Ameryeen, H.A., Campo, P.P., Khan, A.R., Pathan, J.M., 2019. Physical and dynamical parameters of the triple stellar system: HIP109951. *Astrophys. Bull.* 74 (4), 464–474. <https://doi.org/10.1134/S1990341319040126>, arXiv:1911.09972.

Mendez, R., Tokovinin, A., Horch, E., 2018. A speckle survey of southern hipparcos visual doubles and geneva-copenhagen spectroscopic binaries. *RMxAC* 50, 56–57.

Moe, M., Kratter, K.M., 2018. Dynamical formation of close binaries during the pre-main-sequence phase. *Astrophys. J.* 854 (1), 44. <https://doi.org/10.3847/1538-4357/aaa6d2>, arXiv:1706.09894.

Mullaney, J., 2006. Double and Multiple Stars, and How to Observe Them. Springer Science and Business Media.

Naoz, S., Farr, W.M., Lithwick, Y., Rasio, F.A., Teyssandier, J., 2013. Secular dynamics in hierarchical three-body systems. *Mon. Not. R. Astron. Soc.* 431 (3), 2155–2171.

Pecaut, M.J., Mamajek, E.E., 2013. Intrinsic colors, temperatures, and bolometric corrections of pre-main-sequence stars. *Astrophys. J. Suppl. Ser.* 208 (1), 9.

Perryman, M., Lindegren, L., Kovalevsky, J., Hoeg, E., Bastian, U., Bernacca, P., Crézé, M., Donati, F., Grenon, M., Grewing, M. et al., 1997. The hipparcos catalogue.

Prusti, T., De Bruijne, J., Brown, A.G., Vallenari, A., Babusiaux, C., Bailer-Jones, C., Bastian, U., Biermann, M., Evans, D., Eyer, L., et al., 2016. The gaia mission. *Astron. Astrophys.* 595, A1.

Scardia, M., Prieur, J.-L., Pansecchi, L., Ling, J., Argyle, R., Aristidi, E., Zanutta, A., Abe, L., Bendjoya, P., Rivet, J.-P. et al., 2019. Orbital elements of double stars: Ads 12648, ads 12889. *Information Circular- IAU Commission G1 Double Stars*, 199, 3–4.

Schmidt-Kaler, T., 1965. Landolt-bornstein, kh hellwege, ed. Berlin: Springer-Verlag, New Ser., Group, 6, 301.

Stassun, K.G., 2012. Astrophysics: A pas de trois birth for wide binary stars. *Nature* 492 (7428), 191–192.

Sterzik, M.F., Tokovinin, A.A., 2002. Relative orientation of orbits in triple stars. *Astron. Astrophys.* 384 (3), 1030–1037.

Straizys, V., Kurilene, G., 1981. Fundamental stellar parameters derived from the evolutionary tracks. *Astrophys. Space Sci.* 80 (2), 353–368.

Taani, A., Abushattal, A., Khasawneh, A., Almusleh, N., Al-Wardat, M., 2020. Jordan journal of physics. *Jordan J. Phys.* 13 (3), 243–251.

Taani, A., Abushattal, A., Mardini, M.K., 2019a. The regular dynamics through the finite-time lyapunov exponent distributions in 3d hamiltonian systems. *Astron. Nachr.* 340 (9–10), 847–851.

Taani, A., Karino, S., Song, L., Mardini, M., Al-Wardat, M., Abushattal, A., Khasawneh, A., Al-Naimiy, H., 2019b. On the wind accretion model of gx 301–2. *Journal of Physics: Conference Series*, vol. 1258. IOP Publishing, p. 012029.

Tanineah, D.M., Hussein, A.M., Widyan, H., Al-Wardat, M.A., 2023. Trigonometric parallax discrepancies in space telescopes measurements I: The case of the stellar binary system Hip 84976. *Adv. Space Res.* 71 (1), 1080–1088. <https://doi.org/10.1016/j.asr.2022.09.025>.

Tokovinin, A., 1997. Msc-a catalogue of physical multiple stars. *Astron. Astrophys. Suppl. Ser.* 124 (1), 75–84.

Tokovinin, A., 2008. Comparative statistics and origin of triple and quadruple stars., 389(2), 925–938. <https://doi.org/10.1111/j.1365-2966.2008.13613.x>. arXiv:0806.3263.

Tokovinin, A., 2014a. From binaries to multiples. i. data on f and g dwarfs within 67 pc of the sun. *Astron. J.* 147 (4), 86.

Tokovinin, A., 2014b. From binaries to multiples. ii. hierarchical multiplicity of f and g dwarfs. *Astron. J.* 147 (4), 87.

Tokovinin, A., 2017. Orbit alignment in triple stars. *Astrophys. J.* 844 (2), 103. <https://doi.org/10.3847/1538-4357/aa7746>, arXiv:1706.00748.

Tokovinin, A., 2018. Spectroscopic orbits of subsystems in multiple stars. iii. *Astron. J.* 156 (2), 48.

Tokovinin, A., 2020. Close binaries in hierarchical stellar systems. *Contrib. Astron. Obser. Skalnate Pleso* 50 (2), 448–455. <https://doi.org/10.31577/caosp.2020.50.2.448>.

Tokovinin, A., Mason, B.D., Hartkopf, W.I., Mendez, R.A., Horch, E.P., 2016. Speckle Interferometry at SOAR in 2015. *Astronom. J.* 151 (6), 153. <https://doi.org/10.3847/0004-6256/151/6/153>, arXiv:1603.07596.

Tokovinin, A., Moe, M., 2020. Formation of close binaries by disc fragmentation and migration, and its statistical modelling. 491(4), 5158–5171. <https://doi.org/10.1093/mnras/stz3299>. arXiv:1910.01522.

Toonen, S., Portegies Zwart, S., Hamers, A.S., Bandopadhyay, D., 2020. The evolution of stellar triples. The most common evolutionary pathways. *Astronom. Astrophys.* 640, A16. <https://doi.org/10.1051/0004-6361/201936835>, arXiv:2004.07848.

Van Leeuwen, F., 1997. The hipparcos mission. *Space Sci. Rev.* 81 (3–4), 201–409.

Videla, M., Mendez, R.A., Claveria, R.M., Silva, J.F., Orchard, M.E., 2022. Bayesian inference in single-line spectroscopic binaries with a visual orbit. *Astron. J.* 163 (5), 220.

Vynatheya, P., Hamers, A.S., Mardling, R.A., Bellinger, E.P., 2022. Algebraic and machine learning approach to hierarchical triple-star stability. *Mon. Not. R. Astron. Soc.* 516 (3), 4146–4155.

Wenger, M., Ochsenbein, F., Egret, D., Dubois, P., Bonnarel, F., Borde, S., Genova, F., Jasniewicz, G., Laloë, S., Lesteven, S., et al., 2000. The simbad astronomical database—the cds reference database for astronomical objects. *Astron. Astrophys. Suppl. Ser.* 143 (1), 9–22.